Engineering optomechanical entanglement via dual-mode cooling with a single reservoir

Zhi-Qiang Liu,[1] Chang-Sheng Hu,[1] Yun-Kun Jiang,[1] Wan-Jun Su,[1] Huaizhi Wu,[1,*] Yong Li,[2] and Shi-Biao Zheng[1,†]

[1]*Fujian Key Laboratory of Quantum Information and Quantum Optics and Department of Physics, Fuzhou University, Fuzhou 350116, People's Republic of China*

[2]*Beijing Computational Science Research Center, Beijing 100193, People's Republic of China*

(Received 18 October 2020; accepted 1 February 2021; published 22 February 2021)

We study reservoir-engineered entanglement for a cascaded bosonic system consisting of three modes, where the adjacent pairs couple to each other via both the beam-splitter interaction and the coherent parametric interaction with the interaction strengths being tunable. We focus on an optomechanical realization of the model by combining a nondegenerate parametric amplifier and an auxiliary cavity. A great steady-state cavity-mechanical entanglement can be achieved by optimizing the ratio of the interaction strengths, where the optomechanical cavity enacts the cold reservoir, simultaneously laser cooling the pair of hybrid modes delocalized over the auxiliary cavity and the mechanical oscillator. In comparison with the case of cooling a single delocalized mode, the dual-mode cooling approach allows one to obtain a greater amount of entanglement with higher cooling efficiencies and to explore strong entanglement in much broader parameter regions, where the rotating-wave approximation fails for the single-mode cooling case. Moreover, we show that the steady-state cavity-mechanical entanglement is robust to the mechanical thermal noise of the high temperature. The improved reservoir engineering approach can potentially be generalized to other bosonic systems with asymmetric beam-splitter and parametric interactions.

DOI: 10.1103/PhysRevA.103.023525

I. INTRODUCTION

Quantum entanglement has been demonstrated for quantum optical systems involving bosonic modes, such as those involving photons, phonons with atomic (or artificial) spins, and trapped ions. In the past decade, much progress has been made in directly coupled bosonic systems [1] and particularly in microwave and optomechanical devices [2], where the radiation-pressure-force induced coupling between the cavity field and the mechanical resonator enables one to study continuous variable entanglement even for macroscopic-scale objects [3–6]. Moreover, experimental progress in fabrication of arrays of nanomechanical or electromechanical resonators has also shown that multiple light and vibrational modes can be coupled [7,8], with the multi-mode coupling being precisely controlled, e.g., in Refs. [9,10]. Entanglement in coupled multimode bosonic systems furthermore allows one to increase the sensitivity of measurement [11] (e.g., high-precision measurements in displacement [12]) and can be used as a key resource for quantum information processing and tests of the fundamental limits of quantum mechanics [13–15]. Thus, the creation and verification of large entanglement for continuous variables, e.g., optomechanical entanglement between light and macroscopic mechanical objects, has been an outstanding goal.

Optomechanical entanglement is normally vulnerable to environmental noises [16–24], which can lead to strong dissipation in both the cavity field and the mechanical object. However, it has recently attracted wide interest in effectively modifying the dissipation by reservoir engineering, which can be realized with an appropriately engineered coupling to a strongly dissipative cold reservoir usually formed by one of the bosonic modes. Dissipation engineering has been proved to be a very promising avenue for obtaining a large degree of entanglement in the context of cavity QED systems [25–29]. By introducing the reservoir engineering approach to three-mode optomechanical systems under a two-tone or four-tone laser driving, people have proposed schemes for generation of strongly squeezed output light and entangled light beams from an optomechanical cavity by engineering the mechanical oscillator cooled close to its ground state into a cold dissipative reservoir [30–34], generation of mechanical squeezing [35], and remote mechanical entanglement by engineering a cold reservoir formed by the electromagnetic field [36]. Very recently, people have experimentally demonstrated engineered macroscopic entanglement between the two mechanical oscillators by explicitly using the dissipative nature of the microwave resonator [37,38]. The steady-state entanglement (between light fields and mechanical objects or between an electromagnetic field and a mechanical mode) achievable via reservoir engineering can surpass the limit of entanglement created by the coherent parametric interaction, which is imposed by the stability condition of the multi-mode system [16,18,24]. However, we note that the previous reservoir-engineering schemes have mainly focused on the single-mode cooling regime [30–34], i.e., only one of the delocalized target modes is exposed to the cold reservoir, or have been limited by the counterrotating interactions so even

*huaizhi.wu@fzu.edu.cn
†sbzheng11@163.com

 ©2021 American Physical Society

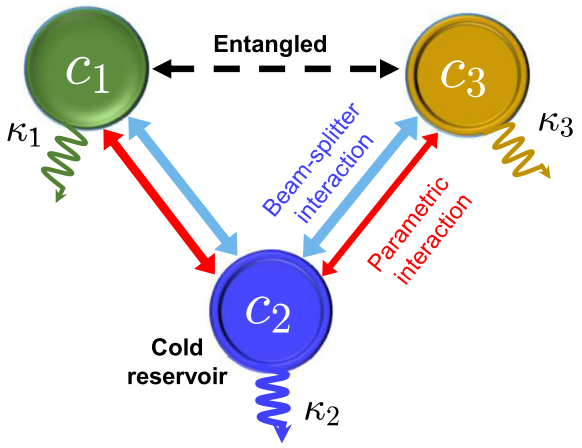

FIG. 1. Sketch of the theoretical model for three bosonic modes interacting via both a beam-splitter interaction and a parametric amplification. The modes c_1 and c_2 are subjected to the two interaction processes with equal weights, while the interaction strengths for the two processes are asymmetric for the modes c_2 and c_3. The mode c_2 is far more dissipative than the other modes and is able to enact as a cold reservoir.

two-mode cooling can potentially be implemented [36,39]. Thus, the schemes have to work in the regime where the rotating-wave approximation is well maintained.

In this paper, we study cavity-mechanical entanglement by reservoir engineering for a generic model consisting of three bosonic modes, as shown in Fig. 1. The couplings between the c_1 and c_2 modes and the c_2 and c_3 modes both involve two interaction mechanisms, i.e., a beam-splitter interaction and a two-mode parametric amplification. The strengths of the two processes are identical for the c_1 and c_2 modes and are unequal for the c_2 and c_3 modes. To mimic the theoretical model, we conceive a hybrid optomechanical setup with a nondegenerate parametric amplifier shared by two coupled cavities: one of which is an auxiliary cavity, and the other is an optomechanical cavity. We find strong and stable steady-state entanglement between the auxiliary cavity field and the mechanical mode by using the optomechanical cavity as a cold dissipative reservoir and by simultaneously cooling the hybridized modes delocalized over both target modes. In contrast to previous reservoir-engineering schemes [30,34], where there exists a dark mode, both the delocalized modes are bright in our model due to the asymmetric weights of the two interaction processes and are only subject to beam-splitter interactions with the optomechanical cavity for a suitable ratio of the weights. As a result, the delocalized modes are simultaneously cooled by the cold dissipative reservoir with different cooling rates, which enables one to generate stronger entanglement between the target modes with higher efficiency in broad parameter regions, which are supposed to have system instability in previous schemes for realizing reservoir-engineered entanglement. In particular, we find that great steady-state entanglement over the bound allowed by a coherent two-mode squeezing interaction can be achieved in the regime far beyond the regular rotating-wave approximation (RWA) condition, thanks to the nonresonant coupling between the reservoir and the target modes. Moreover, the cavity-mechanical entanglement is robust against mechanical thermal noise at high temperature for a large mechanical quality factor. While we focus on the optomechanical realization with the assistance of a nondegenerate parametric amplifier (NDPA), the model may be applied to other three-mode bosonic systems with symmetry breaking interactions.

The paper is arranged as follows. In Sec. II we give a description of our physical model and derive the linearized Hamiltonian for the system. In Sec. III we discuss the reservoir-engineered entanglement between the mechanical oscillator and the auxiliary cavity under the RWA. In Sec. IV, we propose the improved reservoir-engineered method with two-mode cooling and show the strong steady-state cavity-mechanical entanglement without the RWA. Finally, the conclusion is presented in Sec. V.

II. MODEL

We consider a model involving three bosonic modes as shown in Fig. 1(a), which couple to each other via the effective Hamiltonian

$$H = \frac{1}{2}\sum_i E_i c_i^\dagger c_i + \lambda_{12}(c_1^\dagger c_2 + c_1 c_2) + \lambda_{23} c_2^\dagger c_3 + \lambda'_{23} c_2^\dagger c_3^\dagger + \text{H.c.}, \quad (1)$$

where $\lambda_{jk} c_j^\dagger c_k + \text{H.c.}$ $(j \neq k)$ give rise to coherent state (population) transfer between the modes and $\lambda_{jk}^{(\prime)} c_j c_k + \text{H.c.}$ are nondegenerate parametric amplification processes. The modes c_1 and c_2 have equal weights λ_{12} for the state transfer and the parametric process, which for the modes c_2 and c_3 are asymmetric. The model is closely related to multimode opto- and nanomechanical systems [13,40–43], which have recently attracted wide interest for studying the generation of nonclassical states [44,45], nonreciprocal light transmission and amplification [46–49], topological phase transition [50–52], and dynamical synchronization [53–57].

As an example, we envision a hybrid optomechanical setup, which includes a NDPA shared by an auxiliary cavity and an optomechanical cavity with a membrane inside. The NDPA is pumped by a laser at frequency ω_p with the gain Λ, giving rise to pairs of down-converted nondegenerate photons, whose frequencies are resonant with the membrane-free optomechanical cavity and the auxiliary cavity, respectively. The two cavity modes couple with each other via photon hopping with the rate J. While the optomechanical cavity is driven by an external laser with frequency ω_l and driving strength ε, the system Hamiltonian is given by ($\hbar = 1$)

$$H = H_0 + H_{\text{om}} + H_d + H_{a_1 a_2} + H_{\text{NDPA}}, \quad (2)$$

with

$$\begin{aligned} H_0 &= \omega_1 a_1^\dagger a_1 + \omega_2 a_2^\dagger a_2 + \omega_m b^\dagger b, \\ H_{\text{om}} &= g a_1^\dagger a_1 (b^\dagger + b), \\ H_d &= i\varepsilon(a_1^\dagger e^{-i\omega_l t} - a_1 e^{i\omega_l t}), \\ H_{a_1 a_2} &= J(a_1^\dagger a_2 + a_1 a_2^\dagger), \\ H_{\text{NDPA}} &= \Lambda(a_1^\dagger a_2^\dagger e^{-i\omega_p t} + a_1 a_2 e^{i\omega_p t}), \end{aligned} \quad (3)$$

where H_0 includes the free energy of the optomechanical cavity mode a_1, the auxiliary cavity a_2, and the mechanical mode b, which jointly construct the three-mode system described in Eq. (1); $H_{\rm om}$ represents the interaction between the optomechanical cavity and the mechanical membrane induced by the radiation pressure with the single-photon coupling strength g; and H_d describes the longitudinal cavity driving. Assume that the pumping laser has the frequency twice that of the longitudinal driving, i.e., $\omega_p = 2\omega_l$, then the Hamiltonian (3), in the rotating frame with respect to the laser driving frequency ω_l, can be written as

$$\begin{aligned} H' = {} & \Delta_1' a_1^\dagger a_1 + \Delta_2 a_2^\dagger a_2 + \omega_m b^\dagger b + g a_1^\dagger a_1 (b^\dagger + b) \\ & + i\varepsilon(a_1^\dagger - a_1) + \Lambda(a_1^\dagger a_2^\dagger + a_1 a_2) + J(a_1^\dagger a_2 + a_1 a_2^\dagger), \end{aligned} \tag{4}$$

where $\Delta_1' = \omega_1 - \omega_l$ and $\Delta_2 = \omega_2 - \omega_l$ are the detunings of the optomechanical and auxiliary cavity frequencies to the driving laser frequency, respectively. When the dissipation and input noises induced by a Markovian environment are considered, the system dynamics can be studied by the Langevin equation of motion [2],

$$\begin{aligned} \dot{a}_1 = {} & -i\Delta_1' a_1 - i g a_1 (b + b^\dagger) + \varepsilon - i\Lambda a_2^\dagger \\ & - iJ a_2 - \frac{\kappa_1}{2} a_1 + \sqrt{\kappa_1} a_1^{\rm in}, \\ \dot{a}_2 = {} & -i\Delta_2 a_2 - i\Lambda a_1^\dagger - iJ a_1 - \frac{\kappa_2}{2} a_2 + \sqrt{\kappa_2} a_2^{\rm in}, \\ \dot{b} = {} & -i\omega_m b - i g a_1^\dagger a_1 - \frac{\gamma_m}{2} b + \sqrt{\gamma_m} b^{\rm in}, \end{aligned} \tag{5}$$

here κ_j ($j = 1$ and 2) are the cavity decay rates and γ_m is the mechanical damping rate. $a_j^{\rm in}$ and $b^{\rm in}$ are input noise operators for the optical modes (at the vacuum) and the mechanical mode (at thermal temperature T), whose nonzero correlation functions are $\langle a_j^{\rm in}(t) a_j^{\rm in\dagger}(t')\rangle = \delta(t - t')$, $\langle b^{\rm in\dagger}(t) b^{\rm in}(t')\rangle = \bar{n}_b \delta(t - t')$, and $\langle b^{\rm in}(t) b^{\rm in\dagger}(t')\rangle = (\bar{n}_b + 1)\delta(t - t')$ [58,59], where $\bar{n}_b = [\exp(\hbar\omega_m / k_B T) - 1]^{-1}$ is the mean thermal phonon number of the mechanical mode and k_B is the Boltzmann constant.

In the presence of strong coherent driving, we can rewrite the Heisenberg operators as $a_j = \alpha_j + \delta a_j$ and $b = \beta + \delta b$, where δa_j and δb are the quantum fluctuation operators with $\langle \delta a_j \rangle = \langle \delta b \rangle = 0$ around the classical mean values α_j and β, respectively, with $|\alpha_j|, |\beta| \gg 1$. Applying the standard linearization technique to Eq. (5), we then have

$$\begin{aligned} \dot{\alpha}_1 = {} & -i\Delta_1 \alpha_1 - i\Lambda \alpha_2^* - iJ\alpha_2 + \varepsilon - \frac{\kappa_1}{2}\alpha_1, \\ \dot{\alpha}_2 = {} & -i\Delta_2 \alpha_2 - i\Lambda \alpha_1^* - iJ\alpha_1 - \frac{\kappa_2}{2}\alpha_2, \\ \dot{\beta} = {} & -i\omega_m \beta - i g |\alpha_1|^2 - \frac{\gamma_m}{2}\beta, \end{aligned} \tag{6}$$

where $\Delta_1 = \Delta_1' + g(\beta + \beta^*)$ is the effective detuning of the optomechanical cavity to the cavity driving laser, which is modified by the mechanical motion. When the system is in the steady state, the classical mean values are solved as

$$\alpha_1 = \frac{(\xi^* - i2\eta)|u_2|^2}{4\eta^2 - |\xi|^2}\varepsilon, \quad \alpha_2 = \frac{\Lambda\alpha_1^* + J\alpha_1}{-iu_2}, \quad \beta = \frac{g|\alpha_1|^2}{-iu_m}, \tag{7}$$

where $u_1 = i\Delta_1 + \kappa_1/2$, $u_2 = i\Delta_2 + \kappa_2/2$, $u_m = i\omega_m + \gamma_m/2$, $\eta = \Lambda J \Delta_2$, $\xi = u_2\Lambda^2 - u_2^* J^2 - u_1|u_2|^2$, and we have assumed Λ and J are real numbers. Without the NDPA and the auxiliary cavity, one recovers the results $\alpha_1 = \varepsilon/(i\Delta_1 + \kappa_1/2)$ and $\beta = -ig|\alpha_1|^2/(i\omega_m + \gamma_m/2)$ obtained in the standard optomechanical system [16].

Furthermore, by neglecting the higher-order nonlinear terms, the quantum fluctuation operators follow the Langevin equations,

$$\begin{aligned} \delta\dot{a}_1 = {} & -i\Delta_1 \delta a_1 - i g\alpha_1(\delta b + \delta b^\dagger) - i\Lambda \delta a_2^\dagger \\ & - iJ\delta a_2 - \frac{\kappa_1}{2}\delta a_1 + \sqrt{\kappa_1} a_1^{\rm in}, \\ \delta\dot{a}_2 = {} & -i\Delta_2 \delta a_2 - i\Lambda \delta a_1^\dagger - iJ\delta a_1 - \frac{\kappa_2}{2}\delta a_2 + \sqrt{\kappa_2} a_2^{\rm in}, \\ \delta\dot{b} = {} & -i\omega_m \delta b - i g(\alpha_1^* \delta a_1 + \alpha_1 \delta a_1^\dagger) - \frac{\gamma_m}{2}\delta b + \sqrt{\gamma_m} b^{\rm in}, \end{aligned} \tag{8}$$

from which we can readily find the linearized Hamiltonian for the quantum fluctuation operators

$$\begin{aligned} H_{\rm lin} = {} & \sum_{j=1,2} \Delta_j \delta a_j^\dagger \delta a_j + \omega_m \delta b^\dagger \delta b + [G(\delta a_1^\dagger \delta b + \delta a_1 \delta b) \\ & + (\Lambda \delta a_1 \delta a_2 + J \delta a_1 \delta a_2^\dagger) + \text{H.c.}], \end{aligned} \tag{9}$$

where $G = g\alpha_1$ is the cavity-enhanced optomechanical coupling and assumed to be real for simplicity. Now we have constructed the effective Hamiltonian proposed in Eq. (1). The standard optomechanical interaction (i.e., the third term) only leads to symmetric weights for the state transfer and the parametric processes, while the optomechanical-interaction-like Hamiltonian with asymmetric weights is realized by introducing the NDPA and the auxiliary cavity. The Hamiltonian (9) may also be constructed by considering a superconducting circuit realization, where the asymmetric weights can be realized with coupled microwave superconducting cavities with their coupling being modulated by interfacing a superconducting qubit between them [60]. We next show that, by introducing the adjustable weights, the system can be more stable, which remarkably benefits the preparation of steady-state optomechanical entanglement.

III. DISSIPATION-INDUCED OPTOMECHANICAL ENTANGLEMENT UNDER THE RWA

The model can be applied to realize strong optomechanical entanglement between the cavity mode δa_2 and the mechanical mode δb based on the reservoir engineering approach [30,34]. To see the insight, we first set $\Delta_1 = -\Delta_2 = \omega_m$ and $J \approx \Lambda$, and then we recover the three-mode Hamiltonian $H_{\rm lin} = \omega_m(\delta a_1^\dagger \delta a_1 + \beta_1^\dagger \beta_1 - \beta_2^\dagger \beta_2) + g_e(\beta_1 \delta a_1^\dagger + \beta_1^\dagger \delta a_1^\dagger + \text{H.c.})$ by introducing the delocalized Bogoliubov modes $\beta_1 = \delta b \cosh r + \delta a_2^\dagger \sinh r$ and $\beta_2 = \delta a_2 \cosh r + \delta b^\dagger \sinh r$, with $r = \text{arctanh}(\Lambda/G)$ and $g_e = \sqrt{G^2 - \Lambda^2}$ being the effective coupling strength between the cavity mode δa_1 and the delocalized mode β_1. Furthermore, we assume that $G, J \ll 2\omega_m$ and the parametric gain is less than the optomechanical coupling $\Lambda < G$, which allows us to make the RWA and rewrite the linearized

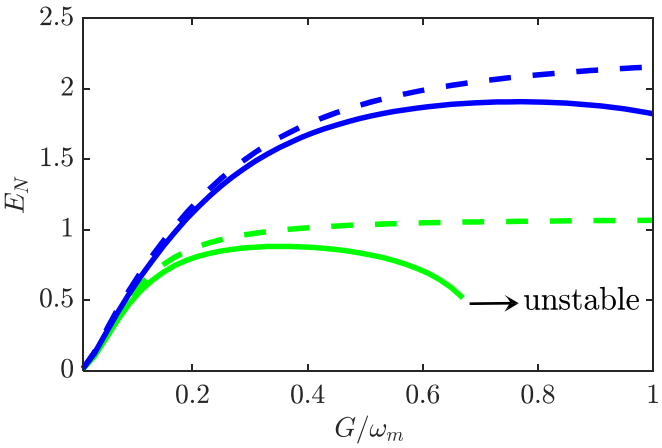

FIG. 2. The steady-state cavity-mechanical entanglement E_N between δb and δa_2 versus the effective optomechanical coupling G/ω_m for $\Lambda/G = 0.9$ (blue, upper lines) and $\Lambda/G = 0.6$ (green, lower lines). The results showing in the solid and dashed lines are simulated by Hamiltonians (9) and (10), respectively. The other parameters are $J = \Lambda$, $\Delta_1 = -\Delta_2 = \omega_m$, $\kappa_1/\omega_m = 0.9$, and $\kappa_2/\omega_m = \gamma_m/\omega_m = 0.01$. The lines are cut off after the onset of the system instability, as indicated by the black arrow. The mechanical thermal noise is not taken into account so far (i.e., $\bar{n}_b = 0$); however, it can be detrimental for the optomechanical entanglement; see Sec. IV for further discussions.

Hamiltonian (9) as [30]

$$H_{\rm lin}^{(\rm R)} = g_e(\beta_1 \delta a_1^\dagger + \beta_1^\dagger \delta a_1). \tag{10}$$

Since the hybridized mode β_2 only dispersively interacts with the optical mode δa_1 for $|J - \Lambda| \ll \omega_m$, one can adiabatically eliminate β_2 under the RWA condition.

The beam-splitter Hamiltonian $H_{\rm lin}^{(\rm R)}$ describes the coherent population transfer between the optical mode δa_1 and the hybridized mode β_1, which cannot generate steady-state entanglement between the two modes β_1 and δa_1, but allows one to effectively realize laser cooling of the hybridized mode β_1 if the optical mode δa_1 is far more dissipative. Since the two-mode squeezed vacuum state $\exp[r(\delta a_2 \delta b - \delta a_2^\dagger \delta b^\dagger)]|0_{a_2}, 0_b\rangle$ is the vacuum for both the delocalized modes β_1 and β_2, thus, when either of the delocalized modes β_1 or β_2 is cooled down to the ground state by the optical mode δa_1 (naturally in its ground state at the room temperature), one can achieve great steady-state entanglement between the cavity mode δa_2 and mechanical mode δb far beyond the bound imposed by using the coherent two-mode squeezing (TMS) interaction Hamiltonian $\hat{H}_{\rm TMS} = \xi \delta a_2 \delta b + \text{H.c.}$, which leads to the steady-state entanglement $E_N^{(\rm TMS)} = \ln(1 + 2\xi/\kappa) \leqslant \ln 2$ limited by the stability condition for $\kappa_2 = \gamma_m = \kappa$ and zero temperature baths, as has been discussed in Refs. [30,34]. Note that strong optomechanical entanglement can be obtained with the state of the hybridized mode β_2 being not at the vacuum [30,34]; see the figures and further discussions in Sec. IV.

By only considering the reduced Hamiltonian (10) and using the logarithmic negativity E_N to measure the two-mode entanglement (see Appendix A), we numerically show in Fig. 2 (the dashed curves) that the steady-state cavity-mechanical entanglement under the case of $\kappa_2 = \gamma_m$ and zero-temperature thermal bath will monotonously increase as G/ω_m varies from 0 to 1 and can saturate at values much larger than the maximum steady-state entanglement $E_N^{(\rm TMS)} \sim \ln 2$ achievable with a coherent two-mode squeezing interaction [30,34]. The steady-state entanglement can be improved by increasing the squeezing parameter r, corresponding to the increase of the ratio Λ/G. However, it should be remembered that $H_{\rm lin}^{(\rm R)}$ is effective only when $G \ll 2\omega_m$ is satisfied, and the full Hamiltonian with counterrotating terms should be considered for $G \geqslant 2\omega_m$. For the typical example with $J = \Lambda$, the steady-state entanglement in this case may decline as G/ω_m dissatisfies the RWA condition, instead of saturation to some values, and the system may become unstable for a larger optomechanical coupling G/ω_m (see the solid curves in Fig. 2).

IV. STRONG AND STABLE OPTOMECHANICAL ENTANGLEMENT BEYOND THE RWA WITH DUAL-MODE COOLING

While great cavity-mechanical entanglement E_N can be obtained by reservoir engineering the delocalized mode β_1, we show that E_N can be modulated and further enhanced by additionally reservoir engineering the "dark" mode β_2. To see the physical insight, we rewrite the full linearized Hamiltonian (9) in terms of the delocalized Bogoliubov modes β_1 and β_2 and have

$$\begin{aligned} H_{\rm lin} = {} & \omega_m(\delta a_1^\dagger \delta a_1 + \beta_1^\dagger \beta_1 - \beta_2^\dagger \beta_2) + g_e(\beta_1 \delta a_1^\dagger + \beta_1^\dagger \delta a_1) \\ & + [g_e - (J - \Lambda)\sinh r](\beta_1^\dagger \delta a_1^\dagger + \beta_1 \delta a_1) \\ & + (J - \Lambda)\cosh r(\beta_2^\dagger \delta a_1 + \beta_2 \delta a_1^\dagger), \end{aligned} \tag{11}$$

which for $J = \Lambda$ reduces to $g_e(\beta_1 \delta a_1^\dagger + \beta_1 \delta a_1) + \text{H.c.}$ For a generic case without making the RWA, the cavity mode δa_1 couples to both β_1 and β_2 due to the asymmetric parametric and beam-splitter interactions between the cavity modes δa_1 and δa_2.

The parametric amplification process for δa_1 and β_1 now has a strength $g_e' \equiv g_e - (J - \Lambda)\sinh r$, which relies on the difference between the NDPA gain and the photon tunneling rate. When $J < \Lambda$, the parametric process becomes stronger than the effective laser cooling process for $g_e' > g_e$, where the system will easily go unstable when the RWA condition $g_e' \ll \omega_m$ is not well satisfied. In contrast, for $\Lambda < J$, there exists an interesting regime where the parametric process can be completely eliminated by setting $J = G^2/\Lambda$ (i.e., $g_e' = 0$), and the interaction Hamiltonian between δa_1 and β_1 remains only the beam-splitter type (10), which leads to fast cooling of the mode β_1 for its resonant coupling with a strong dissipative cavity δa_1.

On the other hand, the asymmetric weights ($J \neq \Lambda$) additionally introduce a nonresonant beam-splitter-like interaction $g_e''(\beta_2^\dagger \delta a_1 + \beta_2 \delta a_1^\dagger)$, with $g_e'' \equiv (J - \Lambda)\cosh r$ and, however, no parametric interaction to the modes δa_1 and β_2. The coherent population transfer from the mode β_2 to the mode δa_1 additionally give rise to ground-state cooling of the hybrid mode β_2 with the cooling rate slower than that of the mode β_1 due to the nonresonant energy gap $2\omega_m$. In general, the simultaneous cooling of the hybrid modes β_1 and β_2 by coupling to a joint "reservoir" δa_1 leads to further

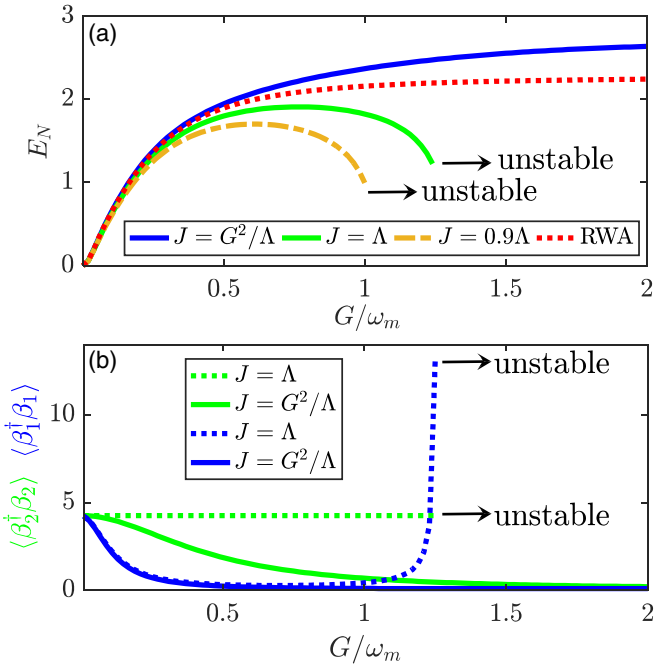

FIG. 3. The steady-state cavity-mechanical entanglement E_N versus the effective optomechanical coupling G/ω_m. The blue solid ($J = G^2/\Lambda$), green solid ($J = \Lambda$) and orange dash-dotted ($J = 0.9\Lambda$) lines are simulated by considering the Hamiltonian (9), and the red dashed line is plotted based on the Hamiltonian (10). (b) Steady-state occupancies of the Bogoliubov modes $\langle\beta_1^\dagger\beta_1\rangle$ (blue lines) and $\langle\beta_2^\dagger\beta_2\rangle$ (green lines) versus G/ω_m for $J = G^2/\Lambda$ (solid lines) and $J = \Lambda$ (dashed lines). Other parameters are the same as those in Fig. 2. The black arrows indicate the unstable regime.

enhancement of the cavity-mechanical entanglement between δa_2 and δb. Remarkably, no counterrotating terms are dropped in our case, and therefore it may allow one to prepare strong and stable cavity-mechanical entanglement beyond the RWA (see further discussion later).

In Fig. 3(a), we show the steady-state cavity-mechanical entanglement E_N between the modes δa_2 and δb with $\Lambda/G = 0.9$ as a function of the effective optomechanical coupling G/ω_m for $J = 0.9\Lambda$ (orange dash-dotted line), $J = \Lambda$ (green solid line), and $J = G^2/\Lambda$ (blue solid line), respectively, and compare them with the case under the RWA (red dashed). For $J = \Lambda$, we can see that the system starts entering into the unstable regime at $G/\omega_m \sim 1.3$. In comparison, by setting $J = 0.9\Lambda$, the system tends to go unstable at a smaller $G/\omega_m \sim 1$ as expected for the case of $J < \Lambda$. Both the two cases generate less cavity-mechanical entanglement than that with the RWA. However, it becomes remarkable when we choose $J = G^2/\Lambda$, where the system remains stable even for $G/\omega_m \sim 2$, and meanwhile, the entanglement achievable is stronger than that under the RWA due to the extra contribution by $(Gg_e/\Lambda)(\delta a_1\beta_2^\dagger + \delta a_1^\dagger\beta_2)$ and thus the simultaneous cooling of the hybrid modes β_1 and β_2.

Assuming that all the localized modes are initially in the vacuum states, and considering the cooling regime $\kappa_2,\ \gamma_m \ll \kappa_1$, the steady-state occupancies of the hybrid modes $\langle\beta_1^\dagger\beta_1\rangle$ and $\langle\beta_2^\dagger\beta_2\rangle$ for $J = G^2/\Lambda$ are shown in Fig. 3(b) and are explicitly given by

$$\begin{aligned}\langle\beta_1^\dagger\beta_1\rangle &= \cosh^2 r\langle\delta b^\dagger\delta b\rangle + \sinh^2 r\langle\delta a_2\delta a_2^\dagger\rangle \\ &\quad + \cosh r\sinh r\langle\delta a_2^\dagger\delta b^\dagger + \delta a_2\delta b\rangle, \\ &\approx \sinh^2 r\frac{C'^2C + [(C+1)+C'C]\xi^2 + 4(C'+1)\xi^4}{2C'^2C + (C+1)^2\xi^2 + 4(C+1)\xi^4},\end{aligned} \tag{12}$$

$$\begin{aligned}\langle\beta_2^\dagger\beta_2\rangle &= \cosh^2 r\langle\delta a_2^\dagger\delta a_2\rangle + \sinh^2 r\langle\delta b\delta b^\dagger\rangle \\ &\quad + \cosh r\sinh r\langle\delta a_2^\dagger\delta b^\dagger + \delta a_2\delta b\rangle, \\ &\approx \sinh^2 r\frac{C'^2C + [(C+1)-C'C]\xi^2 + 4(C+1)\xi^4}{2C'^2C + (C+1)^2\xi^2 + 4(C+1)\xi^4},\end{aligned} \tag{13}$$

with

$$C = \frac{4g_e^2}{\kappa_1\kappa_2},\ C' = \frac{4g_e^2}{\kappa_1^2},\ \xi = \frac{2\omega_m}{\kappa_1},$$

where we have assumed $g_e \approx g_e''$ and $\kappa_2 = \gamma_m$ for simplicity, which are good approximations for the parameter regime in Fig. 3. Considering $J = \Lambda$ (the green lines) for comparison, the nonvanishing parametric process $g_e(\beta_1^\dagger\delta a_1^\dagger + \beta_1\delta a_1)$ gives rise to the exponential growth of $\langle\beta_1^\dagger\beta_1\rangle$ near the critical point of the system instability, and $\langle\beta_2^\dagger\beta_2\rangle$ is invariant since β_2 uncouples to the cavity mode δa_1. While for $J = G^2/\Lambda$, the occupancies of the two hybrid modes $\beta_{1(2)}$ with G/ω_m approaching the regime $C \gg 1$ and $C' \to 1$ are

$$\langle\beta_1^\dagger\beta_1\rangle = \sinh^2 r\frac{C'^2 + (1+C')\xi^2 + 4(C'+1)C^{-1}\xi^4}{2C'^2 + \xi^2(C+4\xi^2)}, \tag{14}$$

$$\langle\beta_2^\dagger\beta_2\rangle = \sinh^2 r\frac{C'^2 + (1-C')\xi^2 + 4\xi^4}{2C'^2 + \xi^2(C+4\xi^2)}, \tag{15}$$

which are first cooled down towards the vacuum due to the coherent population transfer to the "reservoir" mode δa_1, and therefore the cavity-mechanical entanglement increases monotonically as G/ω_m increases to 2 [see Fig. 3(a)]. Note that $\beta_{1(2)}$ could be heated again as G/ω_m further increases, and the occupancies $\langle\beta_{1(2)}^\dagger\beta_{1(2)}\rangle$ will saturate at $\langle\beta_1^\dagger\beta_1\rangle = \langle\beta_2^\dagger\beta_2\rangle = \sinh^2 r/2$ for $C,\ C' \to \infty$.

Moreover, the inequality of the NDPA gain Λ and the photon tunneling rate J allows the system to generate cavity-mechanical entanglement in the parameter region where the RWA (i.e., $g_e \ll \omega_m$) breaks down. In Fig. 4, we show the density plot of E_N versus the effective optomechanical coupling G/ω_m and the ratio Λ/G. Again we first set $J = \Lambda$. In this case, the system with $G \sim 2\omega_m$ can stay in the stable regime only when $\Lambda/G \to 1$, such that the effective coupling $g_e = G\sqrt{1-(\Lambda/G)^2}$ between the modes δa_1 and β_1 safely meets the RWA condition and the parametric amplification for these two modes is well suppressed. In addition, as can be seen in Fig. 4(a), a strong E_N can only be achieved in the vicinity of the unstable region and can thus be sensitive to parametrical fluctuations. In comparison, the stable region of the system with $J = G^2/\Lambda$ expands to the full map of the parameter regime under consideration [see Fig. 4(b)], which

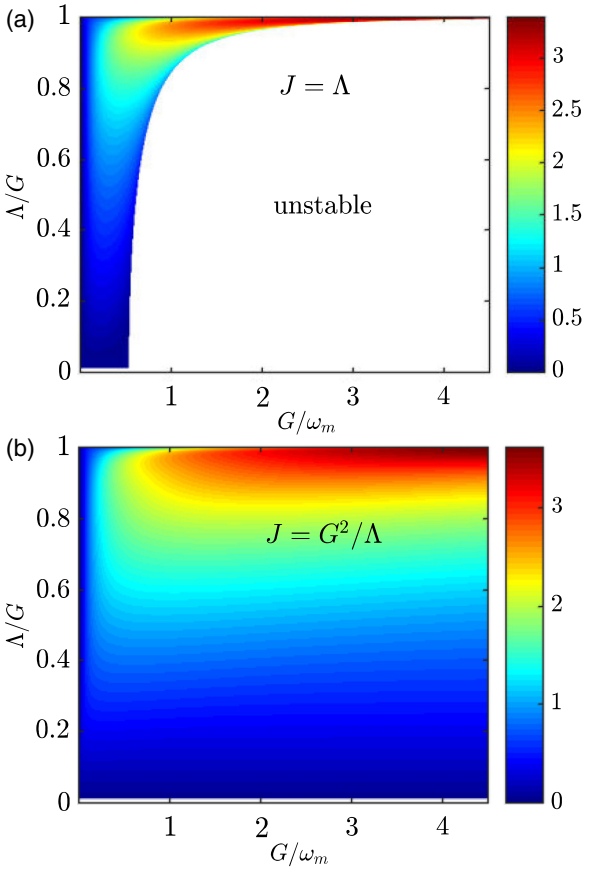

FIG. 4. The steady-state cavity-mechanical entanglement E_N as functions of the effective optomechanical coupling G/ω_m and the ratio Λ/G for (a) $J = \Lambda$ and (b) $J = G^2/\Lambda$. The white region in panel (a) corresponds to the instability of the system. Other parameters are the same as those in Fig. 2.

implies that the strong cavity-mechanical entanglement can be fully controlled for $0 < g_e/G < 1$ even if the strict RWA conditions (i.e., $G/2\omega_m < 1$ and $J/2\omega_m < 1$) are no longer fulfilled.

So far, our discussion has taken $\kappa_2 = \gamma_m$ and zero temperature, corresponding to the generic model (1) with the bosonic modes c_1 and c_3 being completely the same. In this case, the steady-state entanglement E_N for the system being in the stable regime can be improved by simply increasing the ratio κ_1/κ_2, as shown in Fig. 5(a). Here we also find that, by eliminating the heating process $g_e'\beta_1^\dagger \delta a_1^\dagger + \text{H.c.}$ (i.e., setting $J = G^2/\Lambda$), the cooling efficiency for the Bogoliubov modes is further accelerated compared with that for the case of $J = \Lambda$ [19,30], as demonstrated in Fig. 5(b), and a greater steady-state entanglement E_N can be reached.

When a nonzero temperature thermal bath and a different quality factor for the mechanical oscillator are considered, we show the steady-state entanglement with $J = G^2/\Lambda$ as a function of the mean thermal occupancy $\bar{n}_b$ of the mechanical mode b in Fig. 6. It is found that the steady-state entanglement E_N can survive at a high thermal temperature ($T \sim \bar{n}_b\hbar\omega_m$) for a mechanical resonator with a high-quality factor, e.g., for $Q_m^{-1} \equiv \gamma_m/\omega_m = 10^{-4}$, the cavity-mechanical entanglement is robust against a thermal occupation as large

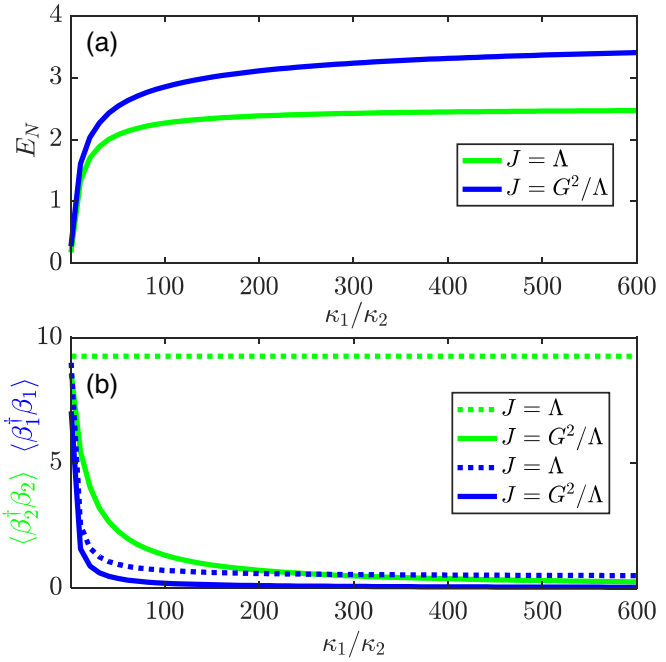

FIG. 5. (a) The steady-state cavity-mechanical entanglement E_N and (b) the occupancies $\langle\beta_1^\dagger\beta_1\rangle$ and $\langle\beta_2^\dagger\beta_2\rangle$ as functions of the decay ratio κ_1/κ_2 for $J = \Lambda$ and $J = G^2/\Lambda$, respectively. Other parameters are $G/\omega_m = 1.5$, $\kappa_1/\omega_m = 0.9$, $\gamma_m/\kappa_2 = 1$, and $\Lambda/G = 0.95$.

as $\bar{n}_b \sim 10^3$. For a practical set of experimental parameters with $\omega_m/2\pi = 5$ MHz, $Q = 10^4$, $m = 50$ ng, $F_1 = 1.7 \times 10^4$, $F_2 = 1.5 \times 10^6$, $L = 1$ mm, and the driving laser of the power $P \simeq 75$ mW and the wavelength $\lambda = 1064$ nm [38,61–63], the cavity-mechanical entanglement can reach $E_N = 3.2$ and can survive even at the thermal temperature $T \simeq 0.96$ K, corresponding to the blue (top) curve in Fig. 6.

Finally, we give a brief discussion on the experimental detection of the cavity-mechanical entanglement. Instead of direct reconstruction of the entire covariance matrix for

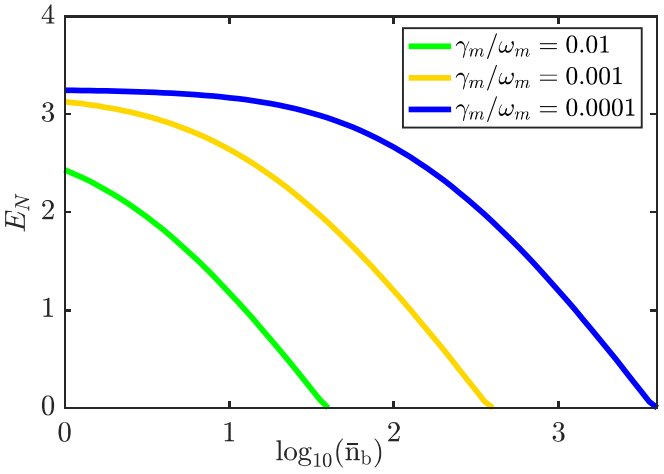

FIG. 6. The steady-state entanglement E_N versus the mean thermal phonon $\bar{n}_b$ of the mechanical mode for $\gamma/\omega_m = 10^{-2}$, $\gamma/\omega_m = 10^{-3}$, and $\gamma/\omega_m = 10^{-4}$, respectively. Other parameters are $G/\omega_m = 1.5$, $\Lambda/G = 0.95$, $J = G^2/\Lambda$, $\kappa_1/\omega_m = 0.9$, and $\kappa_2/\omega_m = 0.01$.

calculating E_N, one can first seek the signature of the steady-state cavity-mechanical entanglement (i.e., $\langle\beta_j^\dagger\beta_j\rangle < \sinh^2 r$, $j = 1$ and 2) in the cavity output spectra based on the Duan's inseparability criterion (see Appendix B) [64]. Considering the strong cavity cooling regime (i.e., $\kappa_1 \gg \kappa_2, \gamma_m$) with $\kappa_2 = \gamma_m$ for simplicity, and supposing that both the optical and the mechanical baths are at the zero temperature [30], we can derive the output spectral density $S_{\rm out}^{(1)}[\omega] = \int dt e^{i\omega t}\langle\delta a_{1,\rm out}^\dagger(t)\delta a_{1,\rm out}(0)\rangle$ of the strong dissipative cavity mode δa_1 in the adiabatic limit, where β_1 and β_2 are decoupled under the condition $2\omega_m \gg (J-\Lambda)G|\chi_1(\omega_m)|$ with $\chi_1(\omega_m) = (i\omega_m + \kappa_1/2)^{-1}$. It follows that

$$S_{\rm out}^{(1)}[\omega_m] = C^{-1}\left[\frac{\kappa_2\langle\beta_1^\dagger\beta_1\rangle}{\kappa_2 + g_e^2\kappa_1|\chi_1(\omega_m)|^2} + \sinh^2 r\right] \tag{16}$$

and

$$S_{\rm out}^{(1)}[-\omega_m] = C^{-1}\left[\frac{\gamma_m\Lambda^2\langle\beta_2^\dagger\beta_2\rangle}{G^2\gamma_m + J^2\kappa_1|\chi_1(\omega_m)|^2} + \sinh^2 r\right]. \tag{17}$$

Thus, the output spectrum $S_{\rm out}^{(1)}[\omega_m]$ at the cavity resonance and $S_{\rm out}^{(1)}[-\omega_m]$ at the frequency detuned by $2\omega_m$ can tell the generation of entanglement. To obtain the degree of entanglement given by the logarithmic negativity, one has to first determine all of the related entries of the covariance matrix. As suggested in Refs. [16,65–67], the quadratures of the cavity mode δa_2 can be directly measured by homodyning the cavity output using a local oscillator, while the mechanical dynamics δq and δp can be measured by resorting to an additional "probe" cavity and observing the output light of it. Thus, by measuring the correlations between the cavity mode and the "probe" cavity, one can in principle obtain all of the entries of the covariance matrix $V(t)$ used to calculate the logarithmic negativity.

V. CONCLUSION

In summary, we have considered a hybrid optomechanical setup with a NDPA and an auxiliary coupled cavity for mimicking a three-mode bosonic system with asymmetric beam-splitter and parametric interactions. By optimizing the parametric gain Λ and the effective optomechanical coupling J such that $J = G^2/\Lambda$, one can efficiently generate the strong steady-state entanglement between the auxiliary cavity and the mechanical oscillator via reservoir engineering, where the optomechanical cavity (i.e., the cold reservoir) is used for effectively laser cooling both the Bogoliubov modes delocalized over the target modes at different cooling rates. The dual-cooling mechanism is applied to engineer the steady-state entanglement in interesting parameter regimes where the RWA is no longer available for a large optomechanical coupling and the system with symmetric beam-splitter and parametric interactions is supposed to be unstable. Our numerical results show that the cavity-mechanical entanglement obtained by the dual-mode cooling can be further improved by increasing the ratio of the dissipation rate for the optomechanical cavity to that for the target modes, and it is robust against the mechanical thermal noise. The improved reservoir engineering scheme can potentially be generalized to speed up cooling and enhance squeezing for multimode bosonic systems with asymmetric couplings.

ACKNOWLEDGMENTS

This work is supported by the National Natural Science Foundation of China under Grants No. 11774058, No. 11674060, No. 11874114, No. 12047524, and No. 11774024; the Natural Science Foundation of Fujian Province under Grant No. 2019J0121; and the Qishan Fellowship of Fuzhou University.

APPENDIX A

To take numerical simulations to verify the strong cavity-mechanical entanglement generated by the reservoir engineering approach, we introduce the position operator $\delta q = (\delta b + \delta b^\dagger)/\sqrt{2}$ and the momentum operator $\delta p = (\delta b - \delta b^\dagger)/i\sqrt{2}$ of the mechanical mode, and the amplitude quadrature $\delta x_j = (\delta a_j + \delta a_j^\dagger)/\sqrt{2}$ and the phase quadrature $\delta y_j = (\delta a_j - \delta a_j^\dagger)/i\sqrt{2}$ of the cavity mode. Using a vector $u = [\delta q, \delta p, \delta x_1, \delta y_1, \delta x_2, \delta y_2]^T$ to include all the quantum fluctuations, Eq. (8) can be expressed as

$$\dot{U} = MU + N, \tag{A1}$$

with

$$M = \begin{pmatrix} -\frac{\gamma_m}{2} & \omega_m & 0 & 0 & 0 & 0 \\ -\omega_m & -\frac{\gamma_m}{2} & -2G & 0 & 0 & 0 \\ 0 & 0 & -\frac{\kappa_1}{2} & \Delta_1 & 0 & -\Lambda + J \\ -2G & 0 & -\Delta_1 & -\frac{\kappa_1}{2} & -\Lambda - J & 0 \\ 0 & 0 & 0 & -\Lambda + J & -\frac{\kappa_2}{2} & \Delta_2 \\ 0 & 0 & -\Lambda - J & 0 & -\Delta_2 & -\frac{\kappa_2}{2} \end{pmatrix},$$

where $N = [\sqrt{\gamma_m}\delta q^{\rm in}, \sqrt{\gamma_m}\delta p^{\rm in}, \sqrt{\kappa_1}\delta x_1^{\rm in}, \sqrt{\kappa_1}\delta y_1^{\rm in}, \sqrt{\kappa_2}\delta x_2^{\rm in}, \sqrt{\kappa_2}\delta y_2^{\rm in}]$ represents the thermal noise source of the system with $\delta q^{\rm in} = (\delta b^{\rm in} + \delta b^{\rm in\dagger})/\sqrt{2}$, $\delta p^{\rm in} = (\delta b^{\rm in} - \delta b^{\rm in\dagger})/i\sqrt{2}$, $\delta x_j^{\rm in} = (\delta a_j^{\rm in} + \delta a_j^{\rm in\dagger})/\sqrt{2}$, and $\delta y_j^{\rm in} = (\delta a_j^{\rm in} - \delta a_j^{\rm in\dagger})/i\sqrt{2}$. The stability condition of the system requires that all eigenvalues of M have negative

real parts, which are associated with the Routh-Hurwitz criterion [68]. Since the input quantum noises are Gaussian, the linearized Hamiltonian can ensure the system is always in the Gaussian state, and the information-related properties can be fully characterized by its 6×6 covariance matrix σ with the matrix elements defined as $\sigma_{jk} = \langle U_j U_k + U_k U_j \rangle / 2$. When the system is in the steady state, σ will be governed by the following Lyapunov equation:

$$M\sigma + \sigma M^T = -D, \tag{A2}$$

where D is a diagonal matrix,

$$D = \mathrm{diag}[\gamma_m(2n_m + 1), \gamma_m(2n_m + 1), \kappa_1, \kappa_1, \kappa_2, \kappa_2]/2, \tag{A3}$$

which is derived by

$$D_{jk}\delta(t - t') = \langle N_j(t)N_k(t') + N_k(t')N_j(t) \rangle / 2. \tag{A4}$$

The entanglement between any pair of bosonic modes can be calculated from the reduced 4×4 covariance matrix $\tilde{\sigma}$, which is extracted from the full 6×6 covariance matrix σ by keeping the components of the corresponding rows and columns [6]. For example, if we intend to calculate the cavity-mechanical entanglement between the cavity mode δa_2 and the mechanical mode δb as in the main text, we simply take out all the elements in the jth rows and the kth columns ($j, k \in \{1, 2, 5, 6\}$) and construct the bipartite covariance matrix $\tilde{\sigma}$ in the following form:

$$\tilde{\sigma} = \begin{pmatrix} S_1 & S_3 \\ S_3^T & S_2 \end{pmatrix}, \tag{A5}$$

where S_1, S_2, and S_3 are 2×2 subblock matrices. The logarithmic negativity E_N used to quantify the cavity-mechanical entanglement is then given by [16,69]

$$E_N = \max[0, -\ln(2\eta^-)], \tag{A6}$$

where $\eta^- \equiv 2^{-1/2}\{\Sigma - [\Sigma^2 - 4\det\tilde{\sigma}]^{1/2}\}^{1/2}$, with $\Sigma = \det S_1 + \det S_2 - 2\det S_3$.

In Fig. 7, we plot steady-state entanglement between any pair of the bosonic modes as the function of Λ/G. Without NDPA ($\Lambda = 0$) and the auxiliary cavity ($J = 0$), and when the standard optomechanical cavity is resonant with the anti-Stokes sideband of the driving laser (i.e., $\Delta_1/\omega_m = 1$), the off-resonant down-conversion process leads to the finite entanglement between the optomechanical cavity and the mechanical mode, i.e., $E_N^{(a_1,b)} \neq 0$ and $E_N^{(a_1,a_2)} = E_N^{(a_2,b)} = 0$. As Λ and J gradually increase, the photon tunneling ($J \neq 0$) from the fast dissipative cavity a_1 to the less dissipative cavity a_2 gives rise to the rise of $E_N^{(a_2,b)}$. Although the parametric interaction $\Lambda(a_1^\dagger a_2^\dagger + a_1 a_2)$ can generate a transient cavity-cavity entanglement, $E_N^{(a_1,a_2)}$, and we may expect the coexistence of all bipartite entanglement between pairs of the modes [70], the steady-state cavity-cavity entanglement $E_N^{(a_1,a_2)}$ is, however, inhibited by the great imbalanced cavity ring-down rates. Moreover, $E_N^{(a_1,b)}$ vanishes for $\Lambda/G \sim 0.53$, and only the cavity-mechanical entanglement $E_N^{(a_2,b)}$ survives and is remarkably strong, which is associated with the reservoir engineering regime and is studied in detail in the main text.

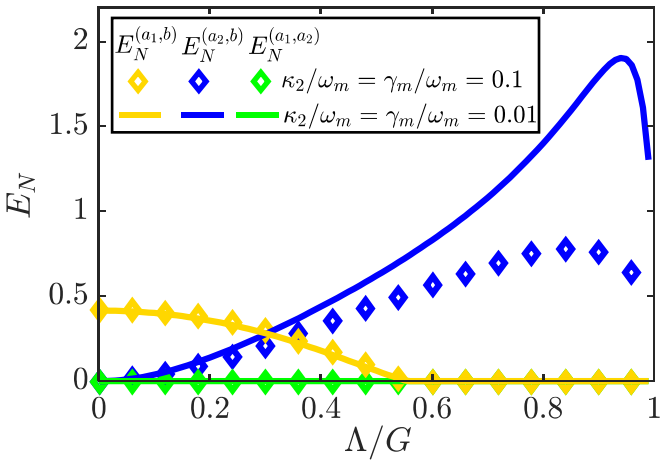

FIG. 7. The steady-state bipartite entanglement $E_N^{(a_1,b)}$, $E_N^{(a_2,b)}$, and $E_N^{(a_1,a_2)}$ in the three-mode (i.e., a_1, a_2, and b) system as the function of the ratio Λ/G for $\kappa_2/\omega_m = 0.1$ (solid line) and $\kappa_2/\omega_m = 0.01$ (labeled), simulated by the full Hamiltonian Eq. (9). Parameters are $\omega_m = 1$, $\Delta_1 = -\Delta_2 = \omega_m$, $G/\omega_m = 0.5$, $J = \Lambda$, $\kappa_1/\omega_m = 0.9$, $\gamma_m = \kappa_2$, and $\bar{n}_b = 0$.

APPENDIX B

From the perspective of experiment, the Duan' s inseparability criterion can provide a simpler method to determine whether there exists entanglement between the two continuous-variable modes δb and δa_2 [64]. In our case, the Duan' s inseparability criterion is expressed as [30]

$$\begin{aligned} D &\equiv \left\langle \left(a\delta q + \frac{1}{a}\delta x_2 \right)^2 \right\rangle + \left\langle \left(a\delta p - \frac{1}{a}\delta y_2 \right)^2 \right\rangle \\ &= a^2 V_{11} + \frac{1}{a^2} V_{22} + C_{12} + C_{12}^* \geqslant \frac{1}{a^2} + a^2, \end{aligned} \tag{B1}$$

with $V_{11} \equiv \langle\{\delta b^\dagger, \delta b\}\rangle$, $V_{22} \equiv \langle\{\delta a_2^\dagger, \delta a_2\}\rangle$, and $C_{12} = \langle\{\delta a_2, \delta b\}\rangle$, where $\{\cdots\}$ denotes the anticommutator. The inequality (B1) is violated when the cavity mode δa_2 and the mechanical mode δb are entangled. Considering the delocalized modes β_1 and β_2 and setting $a^2 = \cosh r/\sinh r = G/\Lambda$, we then have

$$\begin{aligned} \langle\{\beta_1^\dagger, \beta_1\}\rangle &\equiv 1 + 2\langle\beta_1^\dagger\beta_1\rangle \\ &= \frac{\sinh 2r}{2}\left(V_{11}a^2 + V_{22}\frac{1}{a^2} + C_{12} + C_{12}^* \right), \end{aligned} \tag{B2}$$

$$\begin{aligned} \langle\{\beta_2^\dagger, \beta_2\}\rangle &= 1 + 2\langle\beta_2^\dagger\beta_2\rangle \\ &= \frac{\sinh 2r}{2}\left(\frac{1}{a^2}V_{11} + a^2 V_{22} + C_{12} + C_{12}^* \right). \end{aligned} \tag{B3}$$

By applying the Duan' s inseparability criterion, we therefore conclude that either $\langle\beta_1^\dagger\beta_1\rangle < \sinh^2 r$ or $\langle\beta_2^\dagger\beta_2\rangle < \sinh^2 r$; the two modes δb and δa_2 are entangled.

[1] D. Roy, C. M. Wilson, and O. Firstenberg, Rev. Mod. Phys. **89**, 021001 (2017).
[2] M. Aspelmeyer, T. J. Kippenberg, and F. Marquardt, Rev. Mod. Phys. **86**, 1391 (2014).
[3] R. Riedinger, A. Wallucks, I. Marinković, C. Löschnauer, M. Aspelmeyer, S. Hong, and S. Gröblacher, Nature (London) **556**, 473 (2018).
[4] C. Joshi, J. Larson, M. Jonson, E. Andersson, and P. Öhberg, Phys. Rev. A **85**, 033805 (2012).
[5] J.-Q. Liao, Q.-Q. Wu, and F. Nori, Phys. Rev. A **89**, 014302 (2014).
[6] R.-X. Chen, L.-T. Shen, Z.-B. Yang, H.-Z. Wu, and S.-B. Zheng, Phys. Rev. A **89**, 023843 (2014).
[7] X.-Y. Lü, Y. Wu, J. R. Johansson, H. Jing, J. Zhang, and F. Nori, Phys. Rev. Lett. **114**, 093602 (2015).
[8] M. Zhang, S. Shah, J. Cardenas, and M. Lipson, Phys. Rev. Lett. **115**, 163902 (2015).
[9] T. Faust, J. Rieger, M. J. Seitner, J. P. Kotthaus, and E. M. Weig, Nat. Phys. **9**, 485 (2013).
[10] H. Okamoto, A. Gourgout, C.-Y. Chang, K. Onomitsu, I. Mahboob, E. Y. Chang, and H. Yamaguchi, Nat. Phys. **9**, 480 (2013).
[11] C. Zhao, L. Ju, H. Miao, S. Gras, Y. Fan, and D. G. Blair, Phys. Rev. Lett. **102**, 243902 (2009).
[12] J. M. Dobrindt and T. J. Kippenberg, Phys. Rev. Lett. **104**, 033901 (2010).
[13] M. C. Kuzyk and H. Wang, Phys. Rev. A **96**, 023860 (2017).
[14] C. Jiang, S. Tserkis, K. Collins, S. Onoe, Y. Li, and L. Tian, Phys. Rev. A **101**, 042320 (2020).
[15] F. X. Sun, D. Mao, Y. T. Dai, Z. Ficek, Q. Y. He, and Q. H. Gong, New J. Phys. **19**, 123039 (2017).
[16] D. Vitali, S. Gigan, A. Ferreira, H. R. Böhm, P. Tombesi, A. Guerreiro, V. Vedral, A. Zeilinger, and M. Aspelmeyer, Phys. Rev. Lett. **98**, 030405 (2007).
[17] A. Farace and V. Giovannetti, Phys. Rev. A **86**, 013820 (2012).
[18] A. Mari and J. Eisert, Phys. Rev. Lett. **103**, 213603 (2009).
[19] R.-X. Chen, L.-T. Shen, and S.-B. Zheng, Phys. Rev. A **91**, 022326 (2015).
[20] A. Mari and J. Eisert, New J. Phys. **14**, 075014 (2012).
[21] Z.-Q. Yin and Y.-J. Han, Phys. Rev. A **79**, 024301 (2009).
[22] X. Yang, Z. Yin, and M. Xiao, Phys. Rev. A **99**, 013811 (2019).
[23] G. Wang, L. Huang, Y.-C. Lai, and C. Grebogi, Phys. Rev. Lett. **112**, 110406 (2014).
[24] C.-S. Hu, Z.-Q. Liu, Y. Liu, L.-T. Shen, H. Wu, and S.-B. Zheng, Phys. Rev. A **101**, 033810 (2020).
[25] M. B. Plenio and S. F. Huelga, Phys. Rev. Lett. **88**, 197901 (2002).
[26] B. Kraus and J. I. Cirac, Phys. Rev. Lett. **92**, 013602 (2004).
[27] A. S. Parkins, E. Solano, and J. I. Cirac, Phys. Rev. Lett. **96**, 053602 (2006).
[28] B. Kraus, H. P. Büchler, S. Diehl, A. Kantian, A. Micheli, and P. Zoller, Phys. Rev. A **78**, 042307 (2008).
[29] C. A. Muschik, E. S. Polzik, and J. I. Cirac, Phys. Rev. A **83**, 052312 (2011).
[30] Y.-D. Wang and A. A. Clerk, Phys. Rev. Lett. **110**, 253601 (2013).
[31] A. Kronwald, F. Marquardt, and A. A. Clerk, New J. Phys. **16**, 063058 (2014).
[32] Y.-L. Zhang, C.-S. Yang, Z. Shen, C.-H. Dong, G.-C. Guo, C.-L. Zou, and X.-B. Zou, Phys. Rev. A **101**, 063836 (2020).
[33] Z. X. Chen, Q. Lin, B. He, and Z. Y. Lin, Opt. Express **25**, 17237 (2017).
[34] L. Tian, Phys. Rev. Lett. **110**, 233602 (2013).
[35] M. J. Woolley and A. A. Clerk, Phys. Rev. A **89**, 063805 (2014).
[36] R.-X. Chen, C.-G. Liao, and X.-M. Lin, Sci. Rep. **7**, 14497 (2017).
[37] L. D. Tóth, N. R. Bernier, A. Nunnenkamp, A. K. Feofanov, and T. J. Kippenberg, Nat. Phys. **13**, 787 (2017).
[38] C. F. Ockeloen-Korppi, E. Damskägg, J.-M. Pirkkalainen, M. Asjad, A. A. Clerk, F. Massel, M. J. Woolley, and M. A. Sillanpää, Nature (London) **556**, 478 (2018).
[39] C.-G. Liao, R.-X. Chen, H. Xie, and X.-M. Lin, Phys. Rev. A **97**, 042314 (2018).
[40] G. Heinrich, M. Ludwig, H. Wu, K. Hammerer, and F. Marquardt, C. R. Phys. **12**, 837 (2011).
[41] F. Massel, S. U. Cho, J.-M. Pirkkalainen, P. J. Hakonen, T. T. Heikkilä, and M. A. Sillanpää, Nat. Commun. **3**, 987 (2012).
[42] L. Fan, K. Y. Fong, M. Poot, and H. X. Tang, Nat. Commun. **6**, 5850 (2015).
[43] C. F. Ockeloen-Korppi, M. F. Gely, E. Damskägg, M. Jenkins, G. A. Steele, and M. A. Sillanpää, Phys. Rev. A **99**, 023826 (2019).
[44] M. Brunelli, O. Houhou, D. W. Moore, A. Nunnenkamp, M. Paternostro, and A. Ferraro, Phys. Rev. A **98**, 063801 (2018).
[45] R. Zhang, Y. Fang, Y.-Y. Wang, S. Chesi, and Y.-D. Wang, Phys. Rev. A **99**, 043805 (2019).
[46] X.-W. Xu, Y. Li, A.-X. Chen, and Y.-X. Liu, Phys. Rev. A **93**, 023827 (2016).
[47] A. Metelmann and A. A. Clerk, Phys. Rev. X **5**, 021025 (2015).
[48] M. Hafezi and P. Rabl, Opt. Express **20**, 7672 (2012).
[49] L. M. de Lépinay, B. Pigeau, B. Besga, and O. Arcizet, Nat. Commun. **9**, 1401 (2018).
[50] V. Peano, C. Brendel, M. Schmidt, and F. Marquardt, Phys. Rev. X **5**, 031011 (2015).
[51] V. Peano, M. Houde, C. Brendel, F. Marquardt, and A. A. Clerk, Nat. Commun. **7**, 10779 (2016).
[52] C. Sanavio, V. Peano, and A. Xuereb, Phys. Rev. B **101**, 085108 (2020).
[53] M. Zhang, G. S. Wiederhecker, S. Manipatruni, A. Barnard, P. McEuen, and M. Lipson, Phys. Rev. Lett. **109**, 233906 (2012).
[54] A. Mari, A. Farace, N. Didier, V. Giovannetti, and R. Fazio, Phys. Rev. Lett. **111**, 103605 (2013).
[55] P. Djorwé, Y. Pennec, and B. Djafari-Rouhani, Phys. Rev. B **102**, 155410 (2020).
[56] J. Sheng, X. Wei, C. Yang, and H. Wu, Phys. Rev. Lett. **124**, 053604 (2020).
[57] F. Bemani, A. Motazedifard, R. Roknizadeh, M. H. Naderi, and D. Vitali, Phys. Rev. A **96**, 023805 (2017).
[58] V. Giovannetti and D. Vitali, Phys. Rev. A **63**, 023812 (2001).
[59] A. A. Clerk, M. H. Devoret, S. M. Girvin, F. Marquardt, and R. J. Schoelkopf, Rev. Mod. Phys. **82**, 1155 (2010).
[60] F. Galve, L. A. Pachón, and D. Zueco, Phys. Rev. Lett. **105**, 180501 (2010).
[61] D. Kleckner, W. Marshall, M. J. A. de Dood, K. N. Dinyari, B.-J. Pors, W. T. M. Irvine, and D. Bouwmeester, Phys. Rev. Lett. **96**, 173901 (2006).
[62] J. D. Thompson, B. M. Zwickl, A. M. Jayich, F. Marquardt, S. M. Girvin, and J. G. E. Harris, Nature (London) **452**, 72 (2008).

[63] I. Shomroni, A. Youssefi, N. Sauerwein, L. Qiu, P. Seidler, D. Malz, A. Nunnenkamp, and T. J. Kippenberg, Phys. Rev. X **9**, 041022 (2019).
[64] L.-M. Duan, G. Giedke, J. I. Cirac, and P. Zoller, Phys. Rev. Lett. **84**, 2722 (2000).
[65] M. Paternostro, D. Vitali, S. Gigan, M. S. Kim, C. Brukner, J. Eisert, and M. Aspelmeyer, Phys. Rev. Lett. **99**, 250401 (2007).
[66] G. DeChiara, M. Paternostro, and G. M. Palma, Phys. Rev. A **83**, 052324 (2011).
[67] J. Li, I. M. Haghighi, N. Malossi, S. Zippilli, and D. Vitali, New J. Phys. **17**, 103037 (2015).
[68] E. X. DeJesus and C. Kaufman, Phys. Rev. A **35**, 5288 (1987).
[69] G. Vidal and R. F. Werner, Phys. Rev. A **65**, 032314 (2002).
[70] C. Genes, D. Vitali, and P. Tombesi, Phys. Rev. A **77**, 050307(R) (2008).